

1 **Gene-level, but not chromosome-wide, divergence between a very young**
2 **house fly Y chromosome and its homologous X chromosome**

3

4 Jae Hak Son^{1,2,3} and Richard P. Meisel^{1,4}

5

6 1. Department of Biology and Biochemistry, University of Houston, Houston, TX, USA

7

8 2. Current Address: Department of Epidemiology of Microbial Diseases, Yale School of Public
9 Health, New Haven, CT, USA

10

11 3. Jae Hak Son: jaehak.son@yale.edu

12

13 4. Richard P. Meisel: rpmeisel@uh.edu

14 **Abstract**

15

16 X and Y chromosomes are derived from a pair of homologous autosomes, which then diverge
17 from each other over time. Although Y-specific features have been characterized in sex
18 chromosomes of various ages, the earliest stages of Y chromosome evolution are poorly
19 understood. In particular, we do not know whether early stages of Y chromosome evolution
20 consist of changes to individual genes or happen via chromosome-scale divergence from the X.
21 To address this question, we used house fly, *Musca domestica*, as a model because it has very
22 young sex chromosomes that are still segregating as polymorphisms within natural populations.
23 To identify early differentiation between the very young X and Y chromosomes, we compared
24 genotypic (XY) and sex-reversed (XX) males in gene sequence and gene expression using RNA-
25 seq and Oxford Nanopore sequencing data. There is an excess of genes with divergent
26 expression between the X and Y copies, but the number of genes is small. This suggests that
27 individual Y genes, but not the entire Y chromosome, have diverged from their homologous X-
28 linked alleles. We identified one gene, encoding an axonemal dynein assembly factor (which
29 functions in sperm motility), that has higher expression in the abdomens of XY males than XX
30 males because of a disproportionate contribution of the Y allele to gene expression. The up-
31 regulation of the Y-linked copy of this gene may be favored in males because of its function in
32 spermatogenesis, consistent with sexually antagonistic selection affecting the expression
33 evolution of individual genes during early Y chromosome evolution.

34 Introduction

35

36 In many organisms with two separate sexes, a gene on a sex chromosome determines whether an
37 individual develops into a male or female. In XX/XY sex chromosome systems, males are the
38 heterogametic sex (XY genotype), and females are homogametic with the XX genotype (Bull
39 1983). All X and Y chromosomes are ultimately derived from a pair of ancestral autosomes that
40 became sex chromosomes when one homolog obtained a sex-determining locus, such as a male-
41 determining gene on a Y chromosome. The X and Y chromosomes then diverge from each other
42 over time (Bull 1983; Charlesworth et al. 2005). Sex chromosomes have originated and diverged
43 from each other in multiple independent evolutionary lineages (Bachtrog et al. 2014; Beukeboom
44 and Perrin 2014)

45

46 Despite their independent origins, non-homologous Y chromosomes share many common
47 features across species (Charlesworth et al. 2005). First, “masculinization” occurs because male-
48 limited inheritance of the Y chromosome favors the fixation of male-beneficial genetic variants
49 (Rice 1996). Second, suppressed recombination between the X and Y chromosomes evolves,
50 possibly because selection favors co-inheritance of the male-beneficial alleles and the male-
51 determining locus (Charlesworth 2018). Third, “degeneration” occurs in nonrecombining
52 regions; functional genes that were present on ancestral autosomes become pseudogenes on the
53 Y chromosome because suppressed recombination between the X and Y inhibits the purging of
54 deleterious mutations in Y-linked genes (Muller’s ratchet) and enhances the effects of
55 hitchhiking (Charlesworth and Charlesworth 2000; Bachtrog 2013; Vicoso 2019). Other
56 common features of Y chromosomes are repetitive sequences and enlarged heterochromatic
57 regions due to reduced effectiveness of purifying selection caused by suppressed recombination
58 and a small effective population size (Skaletsky et al. 2003). In some cases, a mechanism evolves
59 to compensate for the haploid dosage of X-linked genes in males, but this is not always the case
60 (Mank 2013; Gu and Walters 2017).

61

62 Many features of Y chromosomes are thought to emerge shortly after an autosome becomes Y-
63 linked. For example, recombination suppression has been considered to come after the
64 emergence of a new sex-determining locus on a Y chromosome to favor the co-inheritance of the
65 sex-determining locus and male-beneficial/female-detrimental sexually antagonistic alleles
66 (Orzack et al. 1980; van Doorn and Kirkpatrick 2007; Roberts et al. 2009; van Doorn and
67 Kirkpatrick 2010). As additional sexually antagonistic alleles accumulate on a Y chromosome,
68 this is predicted to trigger progressive spread of the nonrecombining region along the Y
69 chromosome (Rice 1987; van Doorn and Kirkpatrick 2007). Although these features have been
70 characterized in sex chromosomes of various ages and degeneration levels (Bachtrog 2013; Zhou
71 et al. 2014), the very first stages of Y chromosome evolution are poorly understood because of a
72 lack of extremely young sex chromosome systems. Most of the best studied young sex
73 chromosomes have accumulated multiple types of X-Y differentiation, including suppressed
74 recombination, Y chromosome gene loss, or X chromosome dosage compensation (Bergero et al.
75 2013; Mahajan et al. 2018; Darolti et al. 2019; Krasovec et al. 2019). It is therefore unclear the
76 extent to which the early evolution of sex chromosomes is dominated by chromosome-wide X-Y
77 divergence or gene-level differences (Kaiser et al. 2011; Zhou and Bachtrog 2012). This study
78 addresses that shortcoming by determining how a young “proto-Y” chromosome has
79 differentiated from its homologous proto-X chromosome shortly after its emergence.

80

81 We are especially interested in how gene expression differences accumulate between the proto-Y
82 and proto-X chromosomes. As the proto-Y and proto-X chromosomes diverge, it is expected that
83 alleles on the proto-Y chromosome are up- or down-regulated because of *cis*-regulatory sequence
84 differences that contribute to proto-Y gene expression. These *cis*-regulatory effects may be
85 especially important for the expression of sexually antagonistic (male-beneficial/female-
86 deleterious) alleles and degeneration of functional genes (Rice 1984; Zhou and Bachtrog 2012).
87 How these gene expression differences accumulate during the very earliest stages of sex
88 chromosome evolution is not well understood.

89

90 We used the house fly, *Musca domestica*, as a model system to study the early evolution of sex
91 chromosomes because it has very young sex chromosomes that are still segregating as
92 polymorphisms within natural populations (Hamm et al. 2015). The *Musca domestica* male
93 determiner (*Mdmd*) can be found on the Y chromosome (Y^M) and on at least four autosomes
94 (Sharma et al. 2017). Each chromosome carrying *Mdmd*, including Y^M , is a recently derived
95 proto-Y chromosome (Meisel et al. 2017). The proto-Y and proto-X chromosomes show minimal
96 sequence and morphological divergence, as well as similar gene content (Boyes et al. 1964;
97 Hediger et al. 1998; Meisel et al. 2017), consistent with their recent origins. However, it is not
98 clear the extent to which the proto-Y chromosomes are masculinized or degenerated. A previous
99 study revealed a small, but significant, effect of the proto-Y chromosomes on gene expression
100 (Son et al. 2019). However, it could not resolve if the expression differences are the result of
101 changes in the expression of the proto-Y copies, proto-X copies, or both.

102

103 In this study, we tested if one proto-Y chromosome, the third chromosome carrying *Mdmd* (III^M),
104 has evidence of differentiation from its homologous proto-X chromosome by evaluating gene
105 expression and DNA sequence differences between proto-Y genes and their proto-X
106 counterparts. We compared normal (genotypic) males carrying a III^M proto-Y chromosome to
107 sex-reversed males with no proto-Y chromosome using RNA-seq data generated in a previous
108 study (Son et al. 2019) and newly generated Nanopore long read sequencing data. The genotypic
109 males contain one copy each of the proto-Y and proto-X, while the sex-reversed males carry two
110 copies of the proto-X chromosome and no proto-Y. Using sex-reversed males allows us to
111 control for the effect of sexually dimorphic gene expression on the inference of divergence
112 between the proto-Y (III^M) and proto-X. We used these data to test if the early evolution of a Y
113 chromosome is dominated by chromosome-wide or gene-by-gene changes in expression.

114

115

116 **Results and Discussion**

117

118 **DNA sequence divergence between the proto-Y and proto-X chromosomes**

119

120 We used RNA-seq data to identify genetic variants (SNPs and small indels) within genes in
121 genotypic (III^M/III) and sex-reversed (III/III) male house flies (Son et al. 2019). We found that
122 the genotypic males have an excess of heterozygosity on the third chromosome, relative to the
123 sex-reversed males (Figure 1; $P < 10^{-16}$ in a Wilcoxon rank sum test comparing genes on the
124 third chromosome with genes on the other chromosomes). This is consistent with a previous
125 comparison between females and III^M males (Meisel et al. 2017), and it suggests that the

126 sequences of genes on the III^M proto-Y chromosome are differentiated from the copies on the
127 proto-X (i.e., the standard third chromosome).

128
129 We would expect that there would be a similar level of heterozygosity on the ancestral X
130 chromosome in the genotypic males (X/X; III^M/III) and sex-reversed males (X/X; III/III) due to
131 the presence of two copies of the X chromosome in both genotypes. However, the III^M males
132 have elevated heterozygosity on the X chromosome (Figure 1; $P = 8.32 \times 10^{-13}$ in a Wilcoxon rank
133 sum test comparing the X chromosome with chromosomes I, II, IV, and V). This was also
134 observed in a comparison between females and III^M males (Meisel et al. 2017), and the cause of
135 the elevated X chromosome heterozygosity in III^M males remains unresolved.

136 137 **Gene expression divergence between the proto-Y and proto-X chromosomes**

138
139 Elevated heterozygosity on the third chromosome in genotypic (III^M/III) males relative to sex-
140 reversed (III/III) males suggests that the DNA sequences of the house fly III^M proto-Y
141 chromosome is differentiated from the standard third (proto-X) chromosome even if the proto-Y
142 and proto-X chromosomes have similar morphology and gene content (Boyes et al. 1964;
143 Hediger et al. 1998; Meisel et al. 2017). We hypothesized that X-Y sequence differences could
144 contribute to expression differentiation between the proto-Y and the proto-X chromosomes. To
145 test this hypothesis, we quantified differential gene expression between the proto-X and proto-Y
146 chromosome copies of the third chromosome using the RNA-seq data described above and new
147 Oxford Nanopore long read sequencing data.

148
149 We quantified ASE of genes in genotypic (III^M/III) and sex-reversed (III/III) males on the third
150 (proto-sex) chromosome (Figure 2) and the other chromosomes (Supplementary Figure 1). We
151 measured ASE as the proportion of iterations in an MCMC simulation in which the expression of
152 a focal haplotype is estimated as >0.5 (see Materials and Methods). The proportions of iterations
153 with focal haplotypes >0.5 were overrepresented at five points in the histograms (0, 0.25, 0.5,
154 0.75, and 1) both in genotypic and sex-reversed males (Figure 2 and Supplementary Figure 1).
155 These proportions may be overrepresented because we only sampled two genotypes for our ASE
156 analysis, which caused us to have a non-continuous distribution of proportions.

157
158 The proportion of iterations with a focal haplotype >0.5 gives a measure of ASE ranging from 0
159 (extreme ASE in favor of one allele) to 1 (extreme ASE in favor of another allele), with 0.5
160 indicating equal expression of both alleles. We divided our measures of ASE into five bins, with
161 each bin capturing one of the five most common proportions (Figure 2 and Supplementary
162 Figure 1): 1) extreme ASE with a value between 0 and 0.125, 2) moderate ASE with a value
163 between 0.125 and 0.375, 3) no ASE with a value between 0.375 and 0.625, 4) moderate ASE
164 with a value between 0.625 and 0.875, and 5) extreme ASE with a value between 0.875 and 1. In
165 the analysis below, we considered a gene to have ASE if it falls into one of the two bins of
166 extreme ASE, and genes in the no ASE bin were classified as not having no allele-specific
167 expression. Genes with moderate ASE were excluded in order to be conservative about ASE
168 assignment.

169
170 If the III^M proto-Y chromosome is differentiated in gene expression from its homologous III
171 proto-X chromosome because of differences in *cis*-regulatory alleles across the entire third

172 chromosome, then we expect a higher fraction of genes with ASE on the third chromosome in
173 the genotypic (III^M/III) males than in the sex-reversed (III/III) males. In contrast to that
174 expectation, we did not find an excess of genes with ASE in genotypic males compared to ASE
175 genes in sex-reversed males on the third chromosome relative to other chromosomes (Figure 3A
176 and Supplementary Table 1; Fisher's exact test, $P = 0.6996$). This result suggests that the III^M
177 proto-Y chromosome is not broadly differentiated in *cis*-regulatory alleles from the standard
178 third (proto-X) chromosome. This provides evidence that the early stages of Y chromosome
179 evolution do not involve chromosome-wide changes in gene regulation via an excess of *cis*-
180 regulatory mutations.

181
182 We next identified individual genes with differences in ASE between genotypic (III^M/III) and
183 sex-reversed (III/III) males. There are 95 genes with extreme ASE in the genotypic males and no
184 ASE in the sex-reversed males on the third chromosome (Supplementary Table 2). These genes
185 could have ASE in III^M males because of differences in *cis* regulatory sequences between the
186 III^M and standard third chromosome. To test whether the observed number of third chromosome
187 genes with ASE in genotypic males and no ASE in sex-reversed males is in excess of a null
188 expectation, we determined the number of third chromosome genes with no ASE in genotypic
189 males and extreme ASE in sex-reversed males (i.e., the opposite of what we did above to find the
190 first set of 95 genes). There are 76 genes with no ASE in the genotypic males and extreme ASE
191 in the sex-reversed males on the third chromosome (Supplementary Table 2). To test if there is a
192 significant excess of genes with ASE on the third chromosome in III^M males, we also identified
193 241 genes on other chromosomes with ASE in genotypic males and no ASE in sex-reversed
194 males, as well as 281 genes on other chromosomes with no ASE in genotypic males and ASE in
195 sex-reversed males (Figure 3B and Supplementary Table 2). There is an excess of genes (95)
196 with ASE in genotypic males and non-ASE in sex-reversed males compared to the number of
197 genes (76) with non-ASE in genotypic males and ASE in sex-reversed males on the third
198 chromosome, relative to the other chromosomes (Figure 3B and Supplementary Table 2; Fisher's
199 exact test, $P = 0.03467$). These results suggest that, while the III^M proto-Y chromosome is not
200 broadly differentiated in *cis*-regulatory sequences from the standard third (proto-X)
201 chromosome, there is an excess of individual genes with *cis*-regulatory differences between the
202 III^M proto-Y and its homologous proto-X chromosome.

203

204 **Up-regulation of the Y-allele and sex-biased expression**

205

206 Male-beneficial/female-detrimental sexually antagonistic alleles are expected to accumulate on a
207 Y chromosome (Rice 1984). These sexually antagonistic polymorphisms can favor the inhibition
208 of recombination between the male-determining gene and any loci with sexually antagonistic
209 alleles, thereby causing X-Y divergence (van Doorn and Kirkpatrick 2007; van Doorn and
210 Kirkpatrick 2010). One way for alleles to have sexually antagonistic effects is if they are
211 expressed at a level that is beneficial to one sex and deleterious in the opposite sex (Parsch and
212 Ellegren 2013). Alternatively, differential expression of the Y-linked allele from the homologous
213 allele on the X chromosome could be favored after protein-coding sequence divergence between
214 the X and Y alleles that resulted from the fixation of male-beneficial sexually antagonistic alleles
215 in the coding sequence of the Y-linked copy (Mank 2017). In both cases, we expect differential
216 expression between X and Y alleles.

217

218 To test for expression divergence between X and Y copies that are likely to have sex-specific
219 effects, we simultaneously investigated ASE and sex-biased gene expression. Specifically, we
220 tested if genes on the third chromosome with ASE in the genotypic (III^M/III) males and no ASE
221 in the sex-reversed (III/III) males are differentially expressed between genotypic and sex-
222 reversed males. We previously showed that genes with “discordant sex-biased expression” (i.e.,
223 opposite sex-biased expression) between the genotypic and sex-reversed males are over-
224 represented on the third chromosome (Son et al. 2019), suggesting divergence of *cis*-regulatory
225 alleles between the III^M (proto-Y) and standard third (proto-X) chromosomes. However, we did
226 not previously determine which alleles (proto-Y or proto-X copies) are responsible for the
227 expression differences between genotypic and sex-reversed males.

228
229 Using our ASE results, we found one gene (LOC101899975, encoding XM_011293910.2 and
230 XM_011293909.2) with discordant sex-biased gene expression out of the 95 genes on the third
231 chromosome with ASE in the genotypic (III^M/III) males and no ASE in the sex-reversed (III/III)
232 males. This gene is homologous to *dynein assembly factor 5, axonemal* (human gene *DNAAF5*
233 and *Drosophila melanogaster* gene *HEATR2*). The gene, which we refer to as *Musca domestica*
234 *HEATR2* (*Md-HEATR2*), is expected to encode a protein that functions in flagellated sperm
235 motility (Diggle et al. 2014), and it has strong testis-biased expression in *D. melanogaster*
236 (Chintapalli et al. 2007). *Md-HEATR2* has male-biased expression in genotypic males and
237 female-biased expression in sex-reversed males (Son et al. 2019), suggesting that expression
238 differences between the III^M proto-Y and the standard third (proto-X) chromosome cause the
239 male-biased expression of the gene in the genotypic males.

240
241 With haplotypes estimated by IDP-ASE, we identified three diagnostic variant sites for ASE
242 within *Md-HEATR2* (Figure 4A), which are all synonymous SNPs. The genotypic (III^M/III)
243 males are heterozygous and the sex-reversed (III/III) males are homozygous at all diagnostic
244 sites. We inferred the allele on the standard third chromosome as the one in common between
245 genotypic and sex-reversed males, and the III^M allele as the one unique to genotypic males at
246 each diagnostic variant site. *Md-HEATR2* is expressed higher in III^M genotypic males than in
247 sex-reversed males (Figure 4A). In the III^M genotypic males, the III^M (Y-linked) alleles are
248 expressed higher than the X-linked alleles, indicating that the Y-linked alleles are associated with
249 the up-regulation of the gene in III^M genotypic males relative to sex-reversed males (Figure 4A).
250 The copy of *Md-HEATR2* on the III^M proto-Y chromosome is therefore up-regulated relative to
251 the proto-X copy.

252
253 The evolutionary divergence of the proto-X and proto-Y copies of *Md-HEATR2* could constitute
254 an early stage of X-Y differentiation before chromosome-wide X-Y differentiation occurs
255 (Bachtrog 2013). Young Y chromosomes have very similar gene content as their ancestral
256 autosomes, in contrast to old Y chromosomes that have only retained genes with male-specific
257 functions or recruited genes associated with testis expression from other autosomes (Koerich et
258 al. 2008; Kaiser et al. 2011; Mahajan and Bachtrog 2017). Our results suggest that changes in the
259 expression of individual Y-linked genes that were retained from the ancestral autosome could
260 have important phenotypic effects during early Y chromosome evolution, as opposed to
261 chromosome-scale divergence of the proto-Y chromosome from its homologous proto-X
262 chromosome (Zhou and Bachtrog 2012).

263

264 Using Nanopore long read sequencing data, we examined 1,273 base pairs upstream of *Md-*
265 *HEATR2* to identify diagnostic sites that could be responsible for regulating the expression
266 differences between the proto-X and proto-Y alleles. We chose that distance because it includes
267 the first variable site we could identify on the scaffold containing *Md-HEATR2* in our Nanopore
268 data (i.e., including a larger region would not provide any additional information). We found
269 twelve variable sites with different variants (SNPs and small indels) between genotypic (III^M/III)
270 and sex-reversed (III/III) males (Figure 4B). We next examined whether these sites are located
271 within a potential transcription factor (TF) binding region. We found five TF binding regions
272 predicted upstream of *Md-HEATR2* using the ‘Tfsitescan’ tool in the ‘object-oriented
273 Transcription Factors Database (ooTFD)’ (Ghosh 1999). However, none of the twelve variable
274 sites are found within any predicted TF binding regions (Figure 4C). Further work is needed to
275 determine how the differential expression of the proto-X and proto-Y copies of *Md-HEATR2* is
276 regulated.

277
278 If alleles have sexually antagonistic effects (e.g., beneficial to males and deleterious to females),
279 then selection on these alleles could drive sex chromosome turnover if they are tightly linked to a
280 new sex-determining gene (Orzack et al. 1980; van Doorn and Kirkpatrick 2007; Roberts et al.
281 2009; van Doorn and Kirkpatrick 2010). The genetic linkage between sexually antagonistic
282 alleles and the new sex-determining locus could favor restricted or suppressed recombination
283 between the proto-Y and proto-X chromosomes in that linked region, triggering additional X-Y
284 differentiation (Bachtrog 2013). The expression of *Md-HEATR2* could be under sexually
285 antagonistic selection because it functions in flagellated sperm motility (Diggle et al. 2014). *Md-*
286 *HEATR2* has male-biased expression in abdominal tissue (Son et al. 2019), consistent with a
287 function in spermatogenesis. Axonemal dynein is important for male fertility by affecting sperm
288 motility in *Drosophila* (Kurek et al. 1998; Carvalho et al. 2000), suggesting that it may be
289 beneficial to male fitness to have higher expression of *Md-HEATR2*. In addition, investment in
290 expressing the gene in females could be costly, possibly because of the gene’s other functions in
291 mechanosensory neurons (Diggle et al. 2014). Therefore, the up-regulation of *Md-HEATR2* in
292 XY males due to high expression of the proto-Y copy could be consistent with sexually
293 antagonism playing an important role in the early stage of X-Y differentiation at individual genes
294 in house fly.

295 296 **Conclusions**

297
298 We investigated gene sequence and expression differences between the III^M proto-Y and its
299 homologous proto-X chromosome to determine how a very young Y chromosome has been
300 differentiated from its homologous X chromosome shortly after it was formed. To those ends, we
301 used genotypic (III^M/III) and sex-reversed (III/III) males because they are phenotypically almost
302 the same but differ in the proto-sex chromosomes they carry (Hediger et al. 2010; Son et al.
303 2019). We found increased heterozygosity on the III^M proto-Y chromosome in genotypic males
304 relative to sex-reversed males, consistent with sequence divergence between the proto-Y and
305 proto-X (Figure 1). There is not an excess of genes with ASE on the proto-sex chromosome in
306 genotypic males compared to genes with ASE on the same chromosome in sex-reversed males
307 (Figure 3A and Supplementary Table 1). In contrast, we found an excess of individual genes
308 with ASE in the genotypic males and no ASE in the sex-reversed males on the proto-sex
309 chromosome relative to the other chromosomes (Figure 3B and Supplementary Table 2).

310 However, the number of genes with ASE on the third chromosome only in genotypic males, and
311 not in sex-reverse males, is small (<100, which is likely less than 5% of the entire chromosome).
312 We identified one gene on the third chromosome (*Md-HEATR2*) with ASE in genotypic males,
313 no ASE in sex-reversed males, and discordant sex-biased expression between genotypic and sex-
314 reversed males (Figure 4). We hypothesize that expression divergence of *Md-HEATR2* could be
315 an example of very early X-Y differentiation of individual genes that results from sexually
316 antagonistic selection. Therefore, the house fly III^M proto-Y chromosome is differentiated in
317 gene sequence and expression from its homologous proto-X chromosome at individual genes,
318 but not chromosome wide. This suggests that the earliest stages of Y chromosome evolution
319 consist of gene-by-gene, rather than chromosome-scale, changes in gene expression.

320

321

322 **Materials and Methods**

323

324 **Fly strain**

325

326 We analyzed RNA-seq data and performed Oxford Nanopore sequencing on a house fly strain
327 that allows for identification of genotypic (III^M/III) males and sex-reversed (III/III) males
328 (Hediger et al. 2010). This is because the standard third chromosome (III) in this strain has the
329 recessive mutations *pointed wing* (*pw*) and *brown body* (*bwb*). Sex-reversed males (and normal
330 females) have both mutant phenotypes, whereas genotypic males are wild-type for both
331 phenotypes because the III^M chromosome has the dominant wild-type alleles. The RNA-seq data
332 that we analyzed (available at NCBI GEO accession GSE126689) comes from a previous study
333 that used double-stranded RNA (dsRNA) targeting *Md-tra* to create sex-reversed phenotypic
334 males that have a female genotype without a proto-Y chromosome (Son et al. 2019). We
335 compared the sex-reversed males to genotypic males that received a sham treatment of dsRNA
336 targeting GFP. This comparison allows us to investigate genes that have different sex-biased
337 expression in genotypic and sex-reversed males (Son et al. 2019). We used genotypic males and
338 sex-reversed males from the same strain that were subjected to the same treatment for genome
339 sequencing using the Oxford Nanopore long read technology.

340

341 **Oxford Nanopore sequencing**

342

343 We performed Oxford Nanopore sequencing of one genotypic (III^M/III) male and one sex-
344 reversed (III/III) male created in the same strain and using the same *Md-tra* dsRNA treatment as
345 a previous RNA-seq study (Son et al. 2019). DNA was isolated with a phenol/chloroform
346 protocol. A single genotypic male and a single sex-reversed male with detached wings were each
347 transferred to a 1.5 mL Eppendorf tube with 0.5mL homogenization buffer (4.1 g sucrose, 15 mL
348 1M Tris-HCl pH 8.0, 0.5M EDTA, 100 mL dH₂O) and then homogenized using pestles set into a
349 tissue grinder homogenizer. To each tube we added 40 uL of 10% SDS and 2.5 uL of 10mg/mL
350 Proteinase K, and then we incubated the tube at 65°C for 30 min. We next added 2 uL of 4
351 mg/mL RNase to each tube and incubated at 37°C for 15 min. We added 48 uL of 5M KAc to
352 each tube and placed on ice for 30 min. Then we centrifuged the tubes at 14000 rpm for 10 min
353 at 4°C, and the supernatant was transferred into a new tube using a wide-bore pipette tip (all
354 subsequent steps of transfer and mixing during DNA extraction were also done with wide-bore
355 pipette tips to prevent DNA shearing). We added 250 uL phenol and 250 uL chloroform to the

356 extracted supernatant in the new tube, mixed briefly, spun at 14000 rpm for 15 min at 4°C, and
357 then transferred the supernatant into a new tube. We next added 500 uL chloroform to the
358 supernatant in the new tube, mixed well, and spun a 14000 rpm for 5 min at 4°C. We then
359 transferred the supernatant into a new tube. We added 40 uL of 3M NaAc and 800 uL of 95%
360 ethanol to the supernatant in the new tube, mixed briefly, spun at 14000 rpm for 15 min at 4°C,
361 and then carefully poured off all supernatant. We next added 800 uL of 70% ethanol to the
362 remaining pellet, mixed briefly to wash the pellet, spun at 14000 rpm for 15 min at 4°C, removed
363 the supernatant, and then resuspended the pellet in 30 uL of nuclease-free water.

364
365 Oxford Nanopore Sequencing libraries were prepared with the 1D genomic DNA Ligation kit
366 (SQK-LSK109, Oxford Nanopore), following the manufacturer's protocol. DNA from the
367 genotypic male and sex-reversed male (see above) was used to create a separate sequencing
368 library for each genotype. Following the manufacturer's protocol, 15 uL of each library, along
369 with sequencing buffer and loading beads (totaling 75 uL), were loaded onto a R9.4 flow cell
370 until no pores were available on a MinION sequencer (Oxford Nanopore). The libraries from the
371 genotypic and sex-reversed males were run on separate flow cells. Base calling was performed
372 using the Guppy pipeline software version 3.1.5 (Oxford Nanopore) with parameters (--
373 calib_detect --qscore_filtering --min_qscore 10). The base called reads were aligned to the house
374 fly genome assembly v2.0.2 (Scott et al. 2014) using Minimap2 version 2.17 with the "--ax map-
375 ont" parameter (Li 2018).

376 **Variant calling**

377
378 We used available RNA-seq data (Son et al. 2019) to identify genetic variants (SNPs and small
379 insertions/deletions) that differentiate the III^M proto-Y chromosome from the standard third
380 (proto-X) chromosome, and then we tested if III^M males have elevated heterozygosity on the
381 third chromosome as compared to sex-reversed males (Meisel et al. 2017). We used the Genome
382 Analysis Toolkit (GATK) pipeline for calling variants in the RNA-seq data from the *Md-tra*
383 RNAi experiment in (Son et al. 2019), following the best practices for SNP and
384 insertion/deletion (indel) calling on RNA-seq data (McKenna et al. 2010; Meisel et al. 2017). We
385 used STAR (Dobin et al. 2013) to align reads from three genotypic (III^M/III) male libraries and
386 three sex-reversed (III/III) male libraries to the reference assembly v2.0.2 (Scott et al. 2014). The
387 aligned reads were used to generate a new reference genome index from the detected splice
388 junctions in the first alignment run, and then a second alignment was performed with the new
389 reference. We next marked duplicate reads from the same RNA molecule and used the GATK
390 tool 'SplitNCigarReads' to reassign mapping qualities to 60 with the
391 'ReassignOneMappingQuality' read filter for alignments with a mapping quality of 255. Indels
392 were detected and realigned with 'RealignerTargetCreator' and 'IndelRealigner'. The realigned
393 reads were used for base recalibration with 'BaseRecalibrator' and 'PrintReads'. The base
394 recalibration was performed in three sequential iterations in which recalibrated and filtered reads
395 were used to train the next round of base recalibration, at which point there were no beneficial
396 effects of additional base recalibration as verified by 'AnalyzeCovariates'. We next used the
397 recalibrated reads from all three replicates of genotypic and sex-reversed males to call variants
398 using 'HaplotypeCaller' with emission and calling confidence thresholds of 20. We applied
399 'genotypeGVCFs' to the variant calls from the two types of males for joint genotyping, and then
400 we filtered the variants using 'VariantFiltration' with a cluster window size of 35 bp, cluster size
401

402 of 3 SNPs, $FS > 20$, and $QD < 2$. The final variant calls were used to identify heterozygous
403 variants within genes using the coordinates from the genome sequencing project, annotation
404 release 102 (Scott et al. 2014). We measured relative heterozygosity within each gene in
405 genotypic (III^M/III) and sex-reversed (III/III) males as the number of heterozygous variants in
406 genotypic males for a given gene (h_G) divided by the total number heterozygous variants in both
407 genotypic and sex-reversed males (h_{SR}), times one hundred: $100h_G/(h_G + h_{SR})$.

408
409 For the variant calling from Nanopore long reads, the base called reads were indexed using fast5
410 files with the ‘index’ module of Nanopolish version 0.11.1 (Quick et al. 2016), and they were
411 aligned with Minimap2 version 2.17 (Li 2018) to house fly genome assembly v2.0.2 (Scott et al.
412 2014). The aligned and raw reads were used to call variants using the “variants” module of
413 Nanopolish version 0.11.1 with the “--ploidy 2” parameter (Quick et al. 2016). We used a python
414 script ‘nanopolish_makerange.py’ provided in the package to split the genome into 50 kb
415 segments because it was recommended to use the script for large datasets with genome size more
416 than 50 kb.

417 **Allele-specific expression**

418
419 Diploid species can have two alleles at a locus, one of which was inherited maternally and the
420 other paternally. The maternal and paternal alleles can be expressed unequally in the diploid,
421 which is called allele-specific expression (ASE). We investigated if there is elevated ASE on the
422 third chromosome in males carrying one III^M proto-Y and one proto-X chromosome compared to
423 sex-reversed males with two proto-X chromosomes. To do this, we implemented the IDP-ASE
424 tool at the gene level with house fly genome annotation release 102 (Scott et al. 2014), following
425 the developers’ recommended analysis steps (Deonovic et al. 2016). We first prepared
426 information on the number and locations of variants within each gene (SNPs and small indels),
427 as well as read counts at each variant location (see above). The IDP-ASE software was supplied
428 with raw reads and aligned reads created by RNA-seq (Son et al. 2019) and Nanopore
429 sequencing, and variant calls created only by GATK because Nanopore sequencing reads of each
430 library (genotypic male and sex-reversed male) had less than $10 \times$ coverage across the house fly
431 genome (i.e., too low for reliable variant calling).

432
433 The prepared data from each gene was next run in an MCMC (Markov chain Monte Carlo)
434 sampling simulation to estimate the haplotype within each gene with a Metropolis-Hastings
435 sampler (Bansal et al. 2008). Next, the software estimates the proportion of each estimated
436 haplotype that contributes to the total expression of the gene (ρ) from each iteration using slice
437 sampling (Neal and others 2003). A value of $\rho=0.5$ indicates equal expression between two
438 alleles, whereas $\rho<0.5$ or $\rho>0.5$ indicates ASE. The MCMC sampling was run with a 1000
439 iteration burn-in followed by at least 500 iterations where data were recorded. The actual number
440 of iterations was automatically adjusted by the software during the simulation to produce the best
441 simulation output for quantifying ASE within a gene. The IDP-ASE simulation generated a
442 distribution of ρ for each gene across all post-burn-in iterations, and then it calculated the
443 proportion of iterations with $\rho > 0.5$. This proportion was used to estimate the extent of ASE for
444 each gene. For example, if all iterations for a gene have $\rho > 0.5$, then the proportion is 1 and the
445 gene has strong evidence for ASE of one allele. Similarly, if all iterations for a gene have $\rho <$
446 0.5, then the proportion is 0 and the gene has strong evidence for ASE of the other allele. In
447

448 contrast, if half of the iterations have $\rho > 0.5$ and the other half have $\rho < 0.5$, then the proportion
449 is 0.5 and there is not any evidence for ASE. To classify whether genes have ASE or not, we
450 considered only genes with total RNA-seq read counts above 10.

451
452 We used the output of IDP-ASE to compare expression of the III^M (proto-Y) and III (proto-X)
453 alleles in genotypic males. IDP-ASE only quantifies ASE within bi-allelic loci, so we only
454 included genes with heterozygous sites within transcripts in genotypic (III^M/III) or sex-reversed
455 (III/III) males. In addition, we removed heterozygous variants with the same genotype in
456 genotypic and sex-reversed males because they do not allow us discriminate between the proto-Y
457 and proto-X alleles. Removing these variants may have also sped up the simulation times, but
458 this was not rigorously investigated. To discriminate between the III^M and III alleles, we used
459 haplotypes estimated during IDP-ASE runs and genotypes inferred from GATK for genotypic
460 (III^M/III) and sex-reversed (III/III) males. For example, using genotypes called using GATK
461 from the RNA-seq data, we first identified sites with heterozygous alleles in genotypic males and
462 homozygous alleles in sex-reversed males. Next, we inferred the allele in common between
463 genotypic and sex-reversed as the III allele, and the other allele that is unique to genotypic males
464 as the III^M allele. Lastly, we matched those sites to the haplotypes estimated by IDP-ASE to
465 quantify ASE within each genotype.

466
467
468

469 **Acknowledgements and funding information**

470 This work was supported by Grant-in-Aid of Research from the National Academy of Sciences,
471 administered by Sigma Xi, The Scientific Research Society (grant number G2018100198487895
472 to J.H.S. and R.P.M.) and by the National Science Foundation (grant numbers OISE-1444220
473 and DEB-1845686 to R.P.M.). The Oxford Nanopore long reads data used in the study are
474 available from the National Center for Biotechnology Information Sequence Read Archive under
475 BioProject accession PRJNA620357 (BioSample accessions SAMN14518459 for sex-reversed
476 males and SAMN14518460 for genotypic males).

477
478
479

480 **Figure Legends**

481

482 **Figure 1.** Elevated heterozygosity on the third and X chromosomes in genotypic (III^M/III) males
483 relative to sex-reversed (III/III) males. The boxplots show the distributions of the percentages of
484 heterozygous variants within genes on each chromosome in the genotypic males relative to the
485 sex-reversed males. Values more than 50% indicate the increased heterozygosity in genotypic
486 (III^M/III) males, and less than 50% is increased heterozygosity in sex-reversed males. The
487 median across all autosomes is represented by a dashed line.

488

489 **Figure 2.** Histograms of ASE for third chromosome genes in (A) genotypic (III^M/III) and
490 (B) sex-reversed (III/III) males. If a gene is expressed equally between the X and Y alleles, the
491 proportion of focal haplotypes is 0.5; if a gene has ASE, the proportion is greater or less than 0.5.

492

493 **Figure 3.** (A) Proportions of genes with ASE in genotypic (III^M) and sex-reversed (SR) males on
494 each chromosome. (B) Proportions of genes with ASE in genotypic males and non-ASE in sex-
495 reversed males on the third chromosome and all other chromosomes (left two bars). Proportions
496 of genes with non-ASE in genotypic and ASE in sex-reversed males on the third chromosome
497 and all other chromosomes (right two bars).

498

499 **Figure 4.** (A) Diagnostic variable sites for allele-specific expression (ASE) of the *Md-HEATR2*
500 gene based on haplotypes estimated in IDP-ASE; fragments per million mapped reads (FPM).
501 (B) Variable sites that differ between genotypic (III^M) males and sex-reversed males across 1,273
502 base pairs upstream of *Md-HEATR2* using Oxford Nanopore long reads only. The variable sites
503 are marked as triangles with their coordinate as positions in scaffold. (C) Transcription factor
504 (TF) binding motifs predicted within 1,273 base pairs upstream of *Md-HEATR2*.

505 **References**

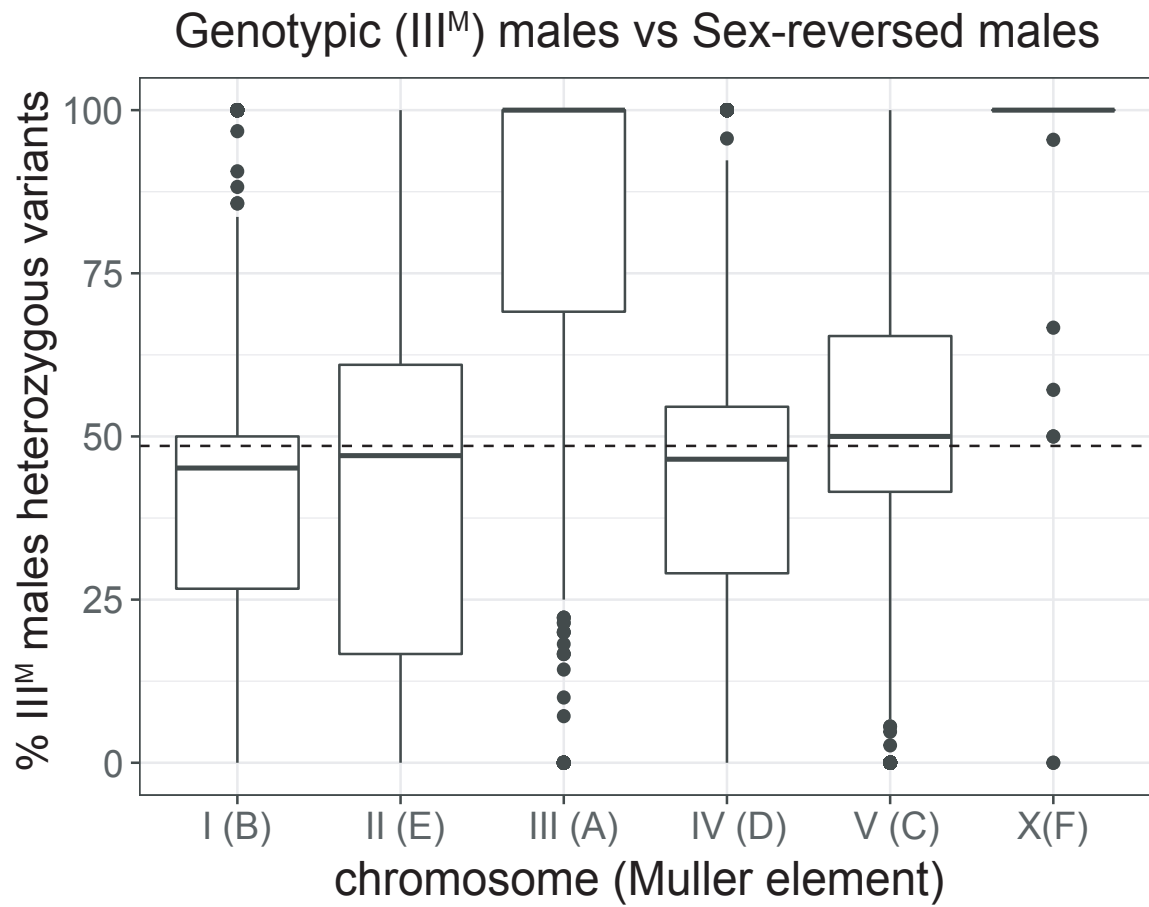
- 506
507 Bachtrog D. 2013. Y-chromosome evolution: emerging insights into processes of Y-chromosome
508 degeneration. *Nat Rev Genet.* 14(2):113.
509
- 510 Bachtrog D, Mank JE, Peichel CL, Kirkpatrick M, Otto SP, Ashman T-L, Hahn MW, Kitano J,
511 Mayrose I, Ming R, et al. 2014. Sex determination: why so many ways of doing it? *PLoS Biol.*
512 12(7):e1001899.
513
- 514 Bansal V, Halpern AL, Axelrod N, Bafna V. 2008. An MCMC algorithm for haplotype assembly
515 from whole-genome sequence data. *Genome Res.* 18(8):1336–1346.
516
- 517 Bergero R, Qiu S, Forrest A, Borthwick H, Charlesworth D. 2013. Expansion of the pseudo-
518 autosomal region and ongoing recombination suppression in the *Silene latifolia* sex
519 chromosomes. *Genetics.* doi:10.1534/genetics.113.150755.
520
- 521 Beukeboom LW, Perrin N. 2014. The evolution of sex determination. Oxford University Press,
522 USA.
523
- 524 Boyes JW, Corey MJ, Paterson HE. 1964. Somatic chromosomes of higher diptera: IX.
525 Karyotypes of some muscid species. *Can J Zool.* 42(6):1025–1036.
526
- 527 Bull JJ. 1983. Evolution of sex determining mechanisms. The Benjamin/Cummings Publishing
528 Company, Inc.
529
- 530 Carvalho AB, Lazzaro BP, Clark AG. 2000. Y chromosomal fertility factors kl-2 and kl-3 of
531 *Drosophila melanogaster* encode dynein heavy chain polypeptides. *Proc Natl Acad Sci.*
532 97(24):13239–13244.
533
- 534 Charlesworth B, Charlesworth D. 2000. The degeneration of Y chromosomes. *Philos Trans R*
535 *Soc London Ser B Biol Sci.* 355(1403):1563–1572.
536
- 537 Charlesworth D. 2018. Does sexual dimorphism in plants promote sex chromosome evolution?
538 *Environ Exp Bot.* doi:10.1016/j.envexpbot.2017.11.005.
539
- 540 Charlesworth D, Charlesworth B, Marais G. 2005. Steps in the evolution of heteromorphic sex
541 chromosomes. *Heredity (Edinb).* 95(2):118.
542
- 543 Chintapalli VR, Wang J, Dow JAT. 2007. Using FlyAtlas to identify better *Drosophila*
544 *melanogaster* models of human disease. *Nat Genet.* doi:10.1038/ng2049.
545
- 546 Darolti I, Wright AE, Sandkam BA, Morris J, Bloch NI, Farré M, Fuller RC, Bourne GR, Larkin
547 DM, Breden F, et al. 2019. Extreme heterogeneity in sex chromosome differentiation and dosage
548 compensation in livebearers. *Proc Natl Acad Sci U S A.* doi:10.1073/pnas.1905298116.
549
- 550 Deonovic B, Wang Y, Weirather J, Wang X-J, Au KF. 2016. IDP-ASE: haplotyping and

- 551 quantifying allele-specific expression at the gene and gene isoform level by hybrid sequencing.
552 *Nucleic Acids Res.* 45(5):e32--e32.
553
- 554 Diggle CP, Moore DJ, Mali G, zur Lage P, Ait-Lounis A, Schmidts M, Shoemark A, Garcia
555 Munoz A, Halachev MR, Gautier P, et al. 2014. HEATR2 Plays a Conserved Role in Assembly
556 of the Ciliary Motile Apparatus. *PLoS Genet.* doi:10.1371/journal.pgen.1004577.
557
- 558 Dobin A, Davis CA, Schlesinger F, Drenkow J, Zaleski C, Jha S, Batut P, Chaisson M, Gingeras
559 TR. 2013. STAR: ultrafast universal RNA-seq aligner. *Bioinformatics.* 29(1):15–21.
560
- 561 van Doorn GS, Kirkpatrick M. 2007. Turnover of sex chromosomes induced by sexual conflict.
562 *Nature.* 449(7164):909.
563
- 564 van Doorn GS, Kirkpatrick M. 2010. Transitions between male and female heterogamety caused
565 by sex-antagonistic selection. *Genetics.* 186(2):629–645.
566
- 567 Ghosh D. 1999. Object oriented transcription factors database (ooTFD). *Nucleic Acids Res.*
568 doi:10.1093/nar/27.1.315.
569
- 570 Gu L, Walters JR. 2017. Evolution of sex chromosome dosage compensation in animals: A
571 beautiful theory, undermined by facts and bedeviled by details. *Genome Biol Evol.*
572 doi:10.1093/gbe/evx154.
573
- 574 Hamm RL, Meisel RP, Scott JG. 2015. The evolving puzzle of autosomal versus Y-linked male
575 determination in *Musca domestica*. *G3 Genes, Genomes, Genet.* 5(3):371–384.
576
- 577 Hediger M, Henggeler C, Meier N, Perez R, Saccone G, Bopp D. 2010. Molecular
578 characterization of the key switch F provides a basis for understanding the rapid divergence of
579 the sex-determining pathway in the housefly. *Genetics.* 184(1):155–170.
580
- 581 Hediger M, Minet AD, Niessen M, Schmidt R, Hilfiker-Kleiner D, Çakir Ş, Nöthiger R,
582 Dübendorfer A. 1998. The male-determining activity on the Y chromosome of the housefly
583 (*Musca domestica* L.) Consists of separable elements. *Genetics.*
584
- 585 Kaiser VB, Zhou Q, Bachtrog D. 2011. Nonrandom gene loss from the drosophila miranda neo-
586 Y chromosome. *Genome Biol Evol.* doi:10.1093/gbe/evr103.
587
- 588 Koerich LB, Wang X, Clark AG, Carvalho AB. 2008. Low conservation of gene content in the
589 *Drosophila* Y chromosome. *Nature.* doi:10.1038/nature07463.
590
- 591 Krasovec M, Kazama Y, Ishii K, Abe T, Filatov DA. 2019. Immediate Dosage Compensation Is
592 Triggered by the Deletion of Y-Linked Genes in *Silene latifolia*. *Curr Biol.*
593 doi:10.1016/j.cub.2019.05.060.
594
- 595 Kurek R, Reugels AM, Glaätzer KH, Bünemann H. 1998. The Y chromosomal fertility factor
596 Threads in *Drosophila hydei* harbors a functional gene encoding an axonemal dynein β heavy

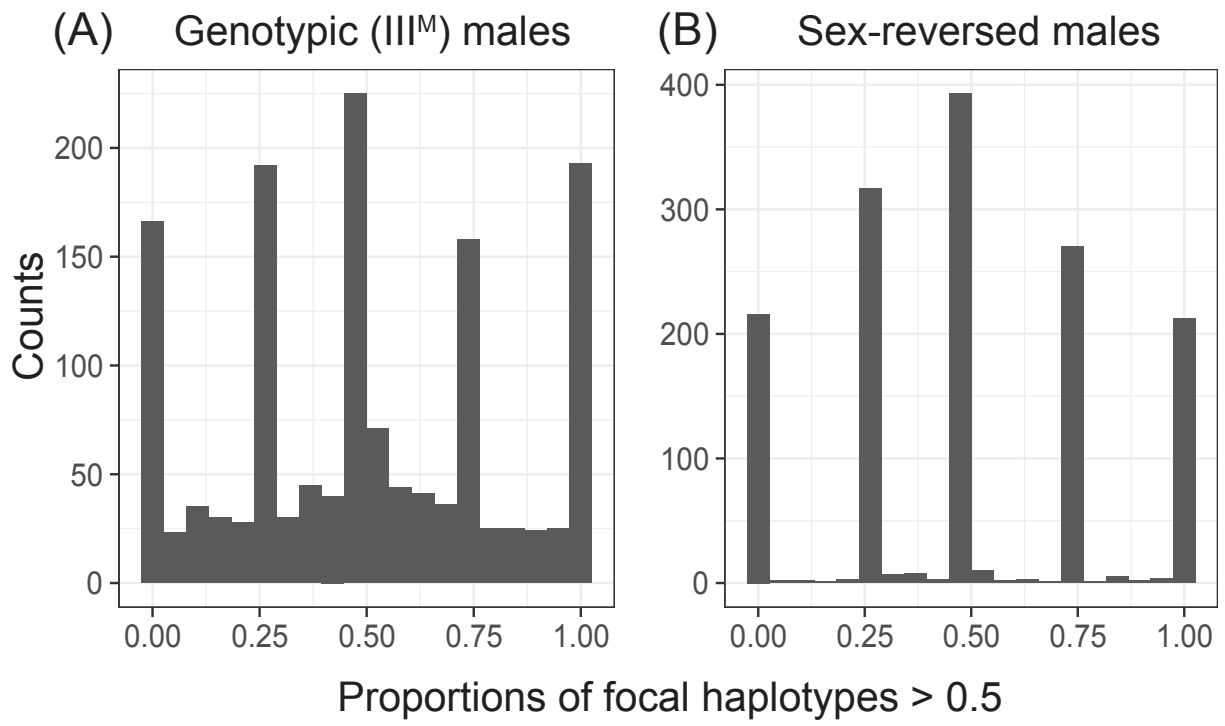
- 597 chain protein. *Genetics*. 149(3):1363–1376.
598
- 599 Li H. 2018. Minimap2: Pairwise alignment for nucleotide sequences. *Bioinformatics*.
600 doi:10.1093/bioinformatics/bty191.
601
- 602 Mahajan S, Bachtrog D. 2017. Convergent evolution of y chromosome gene content in flies. *Nat*
603 *Commun*. doi:10.1038/s41467-017-00653-x.
604
- 605 Mahajan S, Wei KHC, Nalley MJ, Gibilisco L, Bachtrog D. 2018. De novo assembly of a young
606 *Drosophila* Y chromosome using single-molecule sequencing and chromatin conformation
607 capture. *PLoS Biol*. doi:10.1371/journal.pbio.2006348.
608
- 609 Mank JE. 2013. Sex chromosome dosage compensation: Definitely not for everyone. *Trends*
610 *Genet*. doi:10.1016/j.tig.2013.07.005.
611
- 612 Mank JE. 2017. The transcriptional architecture of phenotypic dimorphism. *Nat Ecol Evol*.
613 doi:10.1038/s41559-016-0006.
614
- 615 McKenna A, Hanna M, Banks E, Sivachenko A, Cibulskis K, Kernytsky A, Garimella K,
616 Altshuler D, Gabriel S, Daly M, et al. 2010. The Genome Analysis Toolkit: a MapReduce
617 framework for analyzing next-generation DNA sequencing data. *Genome Res*. 20(9):1297–1303.
618
- 619 Meisel RP, Gonzales CA, Luu H. 2017. The house fly Y Chromosome is young and minimally
620 differentiated from its ancient X Chromosome partner. *Genome Res*. 27(8):1417–1426.
621 Neal RM, others. 2003. Slice sampling. *Ann Stat*. 31(3):705–767.
622
- 623 Orzack SH, Sohn JJ, Kallman KD, Levin SA, Johnston R. 1980. Maintenance of the three sex
624 chromosome polymorphism in the platyfish, *Xiphophorus maculatus*. *Evolution* (N Y).
625 34(4):663–672.
626
- 627 Parsch J, Ellegren H. 2013. The evolutionary causes and consequences of sex-biased gene
628 expression. *Nat Rev Genet*. doi:10.1038/nrg3376.
629
- 630 Quick J, Loman NJ, Duraffour S, Simpson JT, Severi E, Cowley L, Bore JA, Koundouno R,
631 Dudas G, Mikhail A, et al. 2016. Real-time, portable genome sequencing for Ebola surveillance.
632 *Nature*. doi:10.1038/nature16996.
633
- 634 Rice WR. 1984. Sex chromosomes and the evolution of sexual dimorphism. *Evolution* (N Y).
635 38(4):735–742.
636
- 637 Rice WR. 1987. The accumulation of sexually antagonistic genes as a selective agent promoting
638 the evolution of reduced recombination between primitive sex chromosomes. *Evolution* (N Y).
639 41(4):911–914.
640
- 641 Rice WR. 1996. Evolution of the Y sex chromosome in animals. *Bioscience*. 46(5):331–343.
642 Roberts RB, Ser JR, Kocher TD. 2009. Sexual conflict resolved by invasion of a novel sex

643 determiner in Lake Malawi cichlid fishes. *Science* (80-). 326(5955):998–1001.
644
645 Scott JG, Warren WC, Beukeboom LW, Bopp D, Clark AG, Giers SD, Hediger M, Jones AK,
646 Kasai S, Leichter CA, et al. 2014. Genome of the house fly, *Musca domestica* L., a global vector
647 of diseases with adaptations to a septic environment. *Genome Biol.* 15(10):466.
648
649 Sharma A, Heinze SD, Wu Y, Kohlbrenner T, Morilla I, Brunner C, Wimmer EA, van de Zande
650 L, Robinson MD, Beukeboom LW, et al. 2017. Male sex in houseflies is determined by *Mdmd*, a
651 paralog of the generic splice factor gene *CWC22*. *Science* (80-). 356(6338):642–645.
652
653 Skaletsky H, Kuroda-Kawaguchi T, Minx PJ, Cordum HS, Hillier L, Brown LG, Repping S,
654 Pyntikova T, Ali J, Bieri T, et al. 2003. The male-specific region of the human Y chromosome is
655 a mosaic of discrete sequence classes. *Nature.* 423(6942):825.
656
657 Son JH, Kohlbrenner T, Heinze S, Beukeboom LW, Bopp D, Meisel RP. 2019. Minimal effects
658 of proto-Y chromosomes on house fly gene expression in spite of evidence that selection
659 maintains stable polygenic sex determination. *Genetics.* doi:10.1534/genetics.119.302441.
660
661 Vicoso B. 2019. Molecular and evolutionary dynamics of animal sex-chromosome turnover. *Nat*
662 *Ecol Evol.* doi:10.1038/s41559-019-1050-8.
663
664 Zhou Q, Bachtrog D. 2012. Chromosome-wide gene silencing initiates y degeneration in
665 *drosophila*. *Curr Biol.* doi:10.1016/j.cub.2012.01.057.
666
667 Zhou Q, Zhang J, Bachtrog D, An N, Huang Q, Jarvis ED, Gilbert MTP, Zhang G. 2014.
668 Complex evolutionary trajectories of sex chromosomes across bird taxa. *Science* (80-).
669 346(6215):1246338.
670

671 **Figure 1**
672

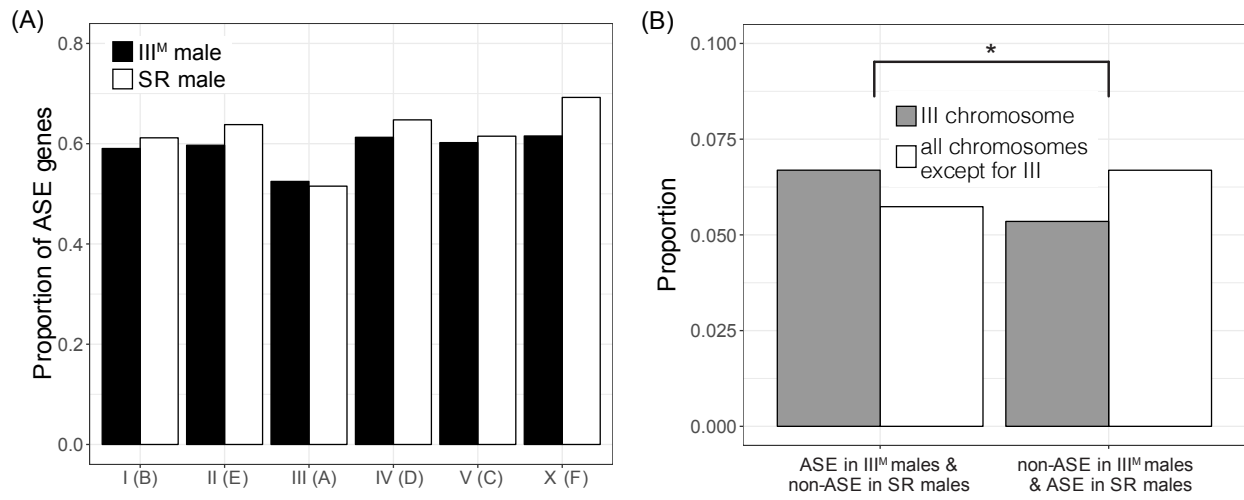


674 **Figure 2**



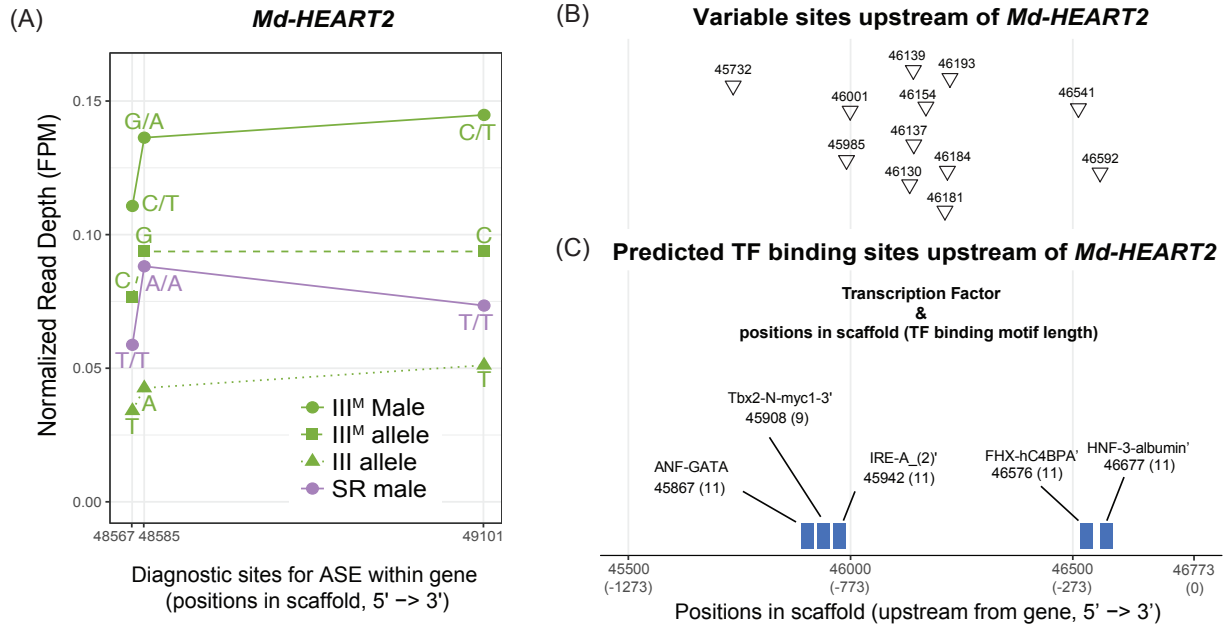
675

676 **Figure 3**
677



678

679 **Figure 4**
680



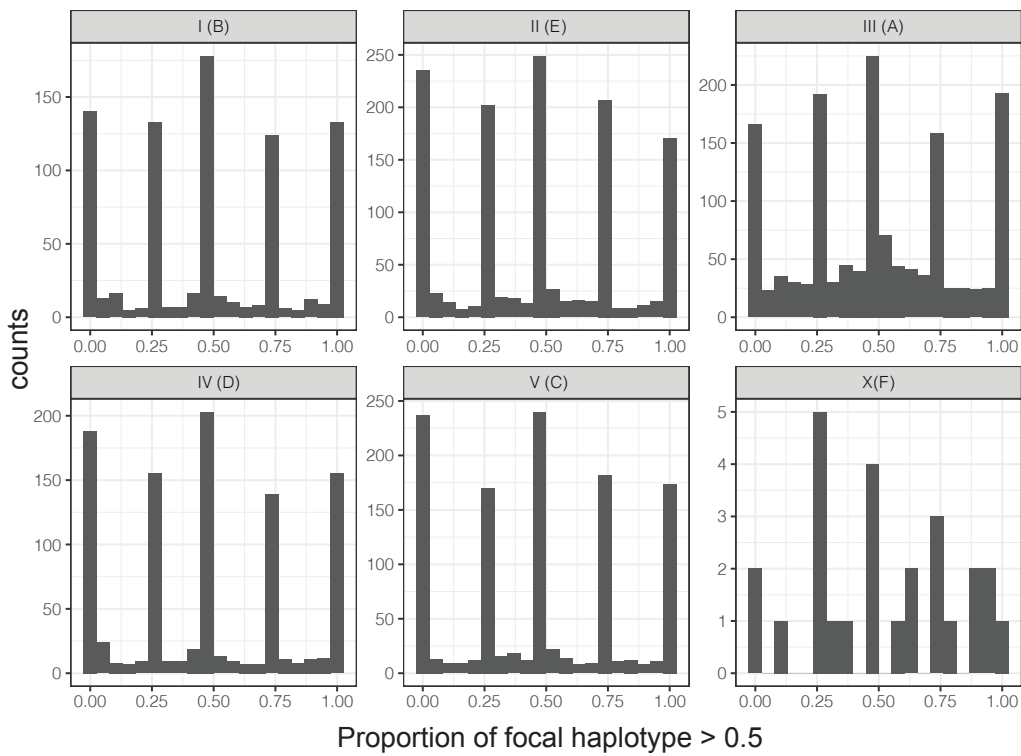
681

682

Supplementary Materials

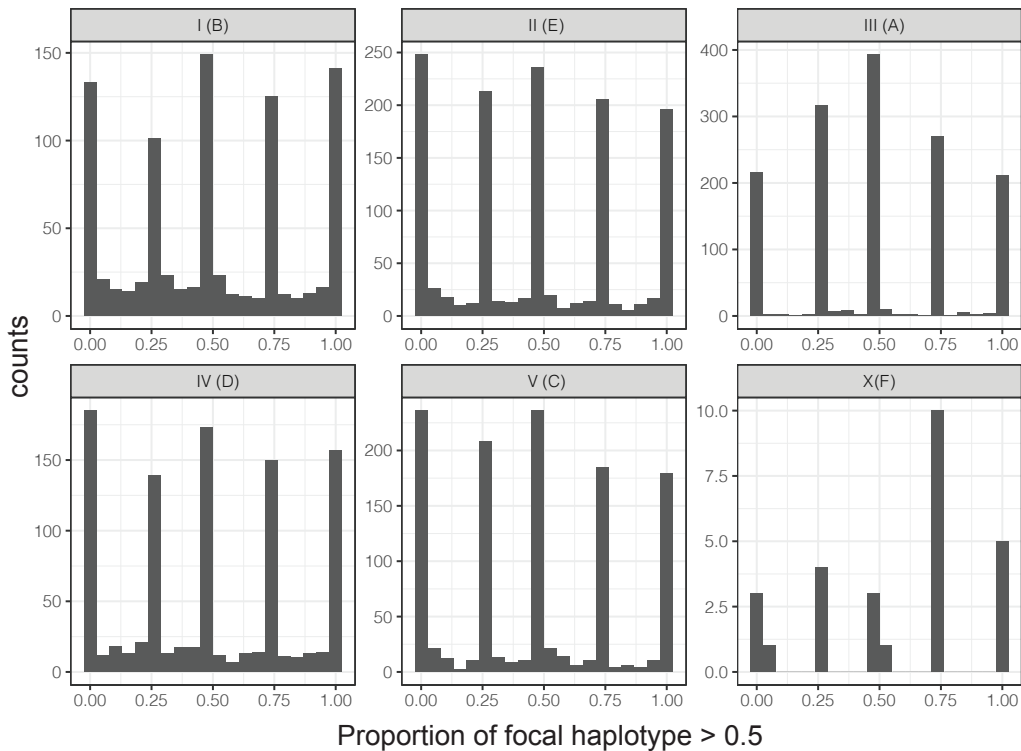
(A)

Genotypic (III^M) males



(B)

Sex-reversed males



683

684 Supplementary Figure 1. Histograms of allele-specific expression (ASE) in genes for all
685 chromosome are shown in the genotypic (III^M/III) males and the sex-reversed (III/III) males.
686 Muller element nomenclature (from *Drosophila*) for each chromosome is given in parentheses. If
687 a gene is expressed equally between two alleles, the proportion of focal haplotype is 0.5;
688 otherwise, the proportion is greater or less than 0.5.

689 Supplementary Table 1. Chromosomal distribution of allele-specific expression (ASE) and no
 690 allele-specific expression (non-ASE) in genotypic (III^M) males and sex-reversed (SR) males.

Chromosome (Muller element)	# genes with ASE in III ^M males	# genes with non-ASE in III ^M males	# genes with ASE in SR males	# genes with non-ASE in SR males	Odds ratio	95% CI of odds ratio
III(A)	456	413	438	412	1.038574	0.8555646 - 1.2606663
genome except III(A)	1635	1089	1711	1010	0.886281	0.7933539 - 0.9900421
I(B)	320	222	334	212	0.915002	0.7123784 - 1.1750187
II(E)	465	314	513	291	0.840134	0.6821523 - 1.0344483
IV(D)	394	249	395	215	0.861373	0.6798614 - 1.0908786
V(C)	448	296	460	288	0.947652	0.7654588 - 1.1730543
X(F)	8	8	9	4	0.720539	0.102255 - 4.754933

691

692 Supplementary Table 2. Counts of genes with ASE on each chromosome in genotypic (III^M)
 693 males and sex-reversed (SR) males. The total number of genes (# genes) in each chromosome
 694 group (second column), # genes with ASE in genotypic males and no ASE in sex-reversed males
 695 (third column), and # genes with no ASE in genotypic males and ASE in sex-reversed males
 696 (fourth column) are shown. Bold indicates statistical significance ($P < 0.05$)

		ASE in III ^M males and non-ASE in SR males	non-ASE in III ^M males and ASE in SR males	Fisher's Exact Test	
Chromosome (Muller element)	# genes	# genes	# genes	Odds ratio compared with III(A)	95% CI
III(A)	1420	95	76		
genome except III(A)	4201	241	281	1.45665	1.014895 - 2.095777
I(B)	824	51	59	1.444139	0.8688985 - 2.4078676
II(E)	1236	68	86	1.578592	0.9961489 - 2.5100267
IV(D)	966	55	76	1.724145	1.063163 - 2.809137
V(C)	1149	67	77	1.434875	0.8982881 - 2.2981210
X(F)	26	0	0	0	0 - Infinity

697

698 Supplementary Table 3. Counts of genes with allele-specific expression (ASE) based on division
 699 of ASE measurements into five sections, following the rules described in the Methods. ASE
 700 proportions are sorted in the order of extreme (1st and 5th), moderate (2nd and 4th), and no (3rd)
 701 ASE. Only extreme ASE was used in the comparisons with no ASE.

Chr (ME)	Sections for ASE proportions	# of genes in genotypic (III ^M /III) Males			# of genes in sex-reversed (III/III) Males		
I (B)	1 st (extreme ASE)	167	320	627	167	334	667
	5 th (extreme ASE)	153			167		
	2 nd (moderate ASE)	158	307		167	333	
	4 th (moderate ASE)	149			166		
	3 rd (no ASE)	222	222		222	212	
II (E)	1 st (extreme ASE)	270	465	972	291	513	1013
	5 th (extreme ASE)	195			222		
	2 nd (moderate ASE)	251	507		258	500	
	4 th (moderate ASE)	256			242		
	3 rd (no ASE)	314	314		314	291	
III (A)	1 st (extreme ASE)	215	456	1043	220	438	1050
	5 th (extreme ASE)	241			218		
	2 nd (moderate ASE)	312	587		333	612	
	4 th (moderate ASE)	275			279		
	3 rd (no ASE)	413	413		413	412	
IV (D)	1 st (extreme ASE)	217	394	754	214	395	794
	5 th (extreme ASE)	177			181		
	2 nd (moderate ASE)	189	360		201	399	
	4 th (moderate ASE)	171			198		
	3 rd (no ASE)	249	249		249	215	
V (C)	1 st (extreme ASE)	258	448	891	268	460	908
	5 th (extreme ASE)	190			192		
	2 nd (moderate ASE)	220	443		239	448	
	4 th (moderate ASE)	223			209		
	3 rd (no ASE)	296	296		296	288	
X(F)	1 st (extreme ASE)	3	8	21	4	9	23
	5 th (extreme ASE)	5			5		
	2 nd (moderate ASE)	7	13		4	14	
	4 th (moderate ASE)	6			10		
	3 rd (no ASE)	5	5		5	4	

702

703

704

705 Supplementary Data 1. A VCF file called with the RNA-seq reads

706 Supplementary Data 2. A VCF file called with the Oxford Nanopore reads

707 Supplementary Data 3. IDP-ASE (allele-specific expression) output for the genotypic males

708 Supplementary Data 4. IDP-ASE (allele-specific expression) output for the sex-reversed males